Biochimica et Biophysica Acta 1808 (2011) 1021–1031

Contents lists available at ScienceDirect

Biochimica et Biophysica Acta

journal homepage: www.elsevier.com/locate/bbamem

A study of the membrane association and regulatory effect of the phospholemman cytoplasmic domain

Eleri Hughes [a], Christopher A.P. Whittaker [a], Igor L. Barsukov [a], Mikael Esmann [b], David A. Middleton [a,*]

[a] School of Biological Sciences, University of Liverpool, Crown Street, Liverpool L69 7ZB, UK
[b] Department of Physiology and Biophysics, Aarhus University, Ole Worms Allé 6, Aarhus, Denmark

ARTICLE INFO

Article history:
Received 12 July 2010
Received in revised form 18 November 2010
Accepted 22 November 2010
Available online 2 December 2010

Keywords:
FXYD
CHIF
Mat-8
Circular dichroism
Isothermal titration calorimetry
Solid-state NMR

ABSTRACT

Phospholemman (PLM) is a single-span transmembrane protein belonging to the FXYD family of proteins. PLM (or FXYD1) regulates the Na,K-ATPase (NKA) ion pump by altering its affinity for K^+ and Na^+ and by reducing its hydrolytic activity. Structural studies of PLM in anionic detergent micelles have suggested that the cytoplasmic domain, which alone can regulate NKA, forms a partial helix which is stabilized by interactions with the charged membrane surface. This work examines the membrane affinity and regulatory function of a 35-amino acid peptide ($PLM_{38–72}$) representing the PLM cytoplasmic domain. Isothermal titration calorimetry and solid-state NMR measurements confirm that $PLM_{38–72}$ associates strongly with highly anionic phospholipid membranes, but the association is weakened substantially when the negative surface charge is reduced to a more physiologically relevant environment. Membrane interactions are also weakened when the peptide is phosphorylated at S68, one of the substrate sites for protein kinases. $PLM_{38–72}$ also lowers the maximal velocity of ATP hydrolysis (V_{max}) by NKA, and phosphorylation of the peptide at S68 gives rise to a partial recovery of V_{max}. These results suggest that the PLM cytoplasmic domain populates NKA-associated and membrane-associated states in dynamic equilibrium and that phosphorylation may alter the position of the equilibrium. Interestingly, peptides representing the cytoplasmic domains of two other FXYD proteins, Mat-8 (FXYD3) and CHIF (FXYD4), have little or no interaction with highly anionic phospholipid membranes and have no effect on NKA function. This suggests that the functional and physical properties of PLM are not conserved across the entire FXYD family.

1. Introduction

Regulation of ion transport, and in particular control of intracellular calcium levels ($[Ca^{2+}]_i$), is essential to muscle function and maintenance of normal patterns of contraction and relaxation. Calcium influx and efflux is coupled to Na^+ and K^+ transport into and out of myocytes, and the entire calcium cycling process is regulated synergistically by several proteins including sarco-endoplasmic reticulum Ca^{2+}-ATPase (SERCA), Na^+,K^+-ATPase (NKA) and the Na^+/Ca^{2+} exchanger (NCX1) [1,2]. NKA and NCX1 are both regulated independently by the 72-residue transmembrane (TM) protein phospholemman (PLM), which is widely distributed in human tissues with expression highest in cardiac and skeletal muscle [3–8]. Disruption of ionic fluxes in cardiac muscle is a contributing factor in heart failure (HF), and myocardial infarction, cardiomyopathy and cardiac hypertrophy all invoke changes in the expression and functions of proteins that maintain the homeostatic norm.

PLM belongs to a group of single-span membrane proteins known as the FXYD family, named in recognition of their invariant Phe-X-Tyr-Asp signature motif close to the N-terminus [9]. FXYD proteins appear to regulate the rate of ion transport across cell membranes via an association with ion pumps. PLM (or FXYD1) is one of at least four members of the family believed to act as a tissue specific regulator of NKA [6,10–12]. PLM associates specifically with the α1/β and α2/β isoforms of NKA, resulting in a small decrease in external K^+ affinity and a nearly two-fold decrease in the internal Na^+ affinity of the enzyme [6], although the precise regulatory effect remains a matter of debate. Regulation of NKA appears to involve contacts between the hydrophobic transmembrane domains of NKA and PLM, with additional interactions in the cytoplasmic regions [13,14]. Measurement of whole-cell NKA currents in the presence of water-soluble peptides representing the 19C-terminal residues of the cytoplasmic domain ($PLM_{54–72}$) indicates that the cytoplasmic domain alone is sufficient to regulate NKA [15]. The cytoplasmic domain of PLM is the major plasma membrane substrate for protein kinase A (PKA) and protein kinase C (PKC) [16,17]. In cardiac muscle, phosphorylation of PLM in the cytoplasmic domain, at S68 alone or at both S68 and S63, occurs following activation of either α or β adrenergic receptors and correlates with an increase in contractility

Abbreviations: PLM, phospholemman (FXYD1); $PLM_{38–72}$, a peptide representing residues 38–72 of phospholemman; Mat-8 (FXYD3), mammary tumor protein; CHIF (FXYD4), corticosteroid induced factor; REDOR, rotational-echo double-resonance; SSNMR, solid-state NMR; ITC, isothermal titration calorimetry; NKA, Na^+,K^+-ATPase; NCX, Na^+/Ca^{2+} exchanger; DMPC, dimyristoylphosphatidylcholine; DOPC, dioleoylphosphatidylcholine; DOPG, dimyristoylphosphatidylglycerol; DOPS, dioleoylphosphatidylserine

* Corresponding author. Tel.: +44 151 7954457.
E-mail address: middleda@liv.ac.uk (D.A. Middleton).

0005-2736/$ – see front matter © 2010 Published by Elsevier B.V.
doi:10.1016/j.bbamem.2010.11.024

[8,16]. Phosphorylation of PLM_{54-72} at S68 stimulates NKA activity to a level above that in the absence of the peptide [15], providing a link between kinase activation and pump modulation.

The three-dimensional structure of PLM in a lipid bilayer environment is not known and the precise nature of its association with NKA is also unclear, although structural models have been proposed [18–20]. NMR structural analysis of PLM in SDS micelles identified two helical segments in the cytoplasmic domain, including an amphipathic helix H4 from residues 59 to 70 which associates with the negatively charged micelle surface and orients approximately perpendicular to the transmembrane region [19,21,22]. Studies of a 35-amino acid peptide representing the PLM cytoplasmic domain (PLM_{38-72}) also revealed strong interactions with the headgroups of negatively charged phospholipids [23]. A recent study found that phosphorylation of PLM at S68 does not alter significantly the structure or dynamics of the cytoplasmic domain in SDS micelles, and increases only slightly the dynamics of the C-terminal helical segment [20]. In the same study it was speculated that the membrane location of H4 allows it to be positioned close to the end of transmembrane helix 10 of NKA, where it could contribute to the network of positive charges constituting a putative voltage-sensing module [20]. The extent to which the structure and dynamics of PLM in detergent micelles emulate its properties in a lipid bilayer has not been established. In view of the functional role of the PLM cytoplasmic domain, studies of its structural and dynamic properties in the presence of lipid bilayers would provide useful new insights into the properties of PLM.

Here we use isothermal titration calorimetry (ITC) and solid-state NMR to examine the interactions of the peptide PLM_{38-72} (sequence shown in Fig. 1) with phospholipid membranes of different head-group composition. We show that the membrane affinity of PLM_{38-72} is highly dependent on membrane surface charge and is reduced after phosphorylation of the peptide at S68. Both peptides lower the rate of ATP hydrolysis by NKA in a kidney membrane preparation, but the S68 phosphorylated peptide has less pronounced inhibitory effect than PLM_{38-72}. Both peptides also lower the affinity for ADP binding to the high-affinity nucleotide binding site. Peptides representing the cytoplasmic domains of two other FXYD family proteins, the 8 kDa mammary tumor protein Mat-8 (FXYD3) and the corticosteroid induced factor CHIF (FXYD4), have much lower membrane affinities than PLM_{38-72} and do not affect NKA activity, suggesting that there is variability in the physical and functional properties amongst the FXYD family members.

2. Methods and materials

2.1. Materials

Synthetic analogues of the human PLM, Mat-8 and CHIF cytoplasmic domains were purchased in pure form (>95%) from Peptide Protein Research Ltd (Fareham, U.K.). PLM_{38-72} and the S68-phosphorylated derivative ($pPLM_{38-72}$) were N-terminally acetylated in order to mimic the internal peptide bond. One batch of PLM_{38-72} was uniformly labeled with ^{13}C and ^{15}N at residues R61, R65, R66 and R67 ($[^{13}C,^{15}N]PLM_{38-72}$). In addition a shorter cytoplasmic fragment (PLM_{63-72}) and an N-terminal extracellular fragment (PLM_{1-12}) containing the FXYD sequence were also prepared. The C-terminus of PLM_{1-12} was amidated to mimic the internal peptide bond of full-length PLM. $pPLM_{38-72}$ was synthesized using the appropriate fmoc-protected phosphoserine precursor and 100% incorporation of the phosphate group was confirmed by electrospray mass spectroscopy and ^{1}H and ^{31}P NMR spectroscopy.

L-α-Dioleoylphosphatidylcholine (DOPC), L-α-dimyristoylphosphatidyl-choline (DMPC), L-α-dioleoylphosphatidylserine (DOPS), L-α-dioleoyl-phosphatidylglycerol (DOPG), and all other chemicals were purchased from Sigma Chemicals Ltd (UK). [^{14}C]ADP with a specific radioactivity of about $2 \cdot 10^{9}$Bq/mmol was obtained from New England Nuclear (USA).

2.2. Preparation of Na,K-ATPase

Membranous NKA from pig kidney microsomal membranes was prepared using SDS and purified by differential centrifugation to a specific activity of about 30 μmol ATP hydrolyzed/mg protein per min at 37 °C [24,25]. Stock solutions of the enzyme were stored at about 5 mg protein/ml in 20 mM histidine, 1 mM EDTA and 250 mM sucrose (pH 7.0). Renal NKA co-purifies with the γ-subunit protein (FXYD2), which is homologous to PLM in the transmembrane domain but lacks the extended cytoplasmic region of PLM. For this latter reason it was assumed that functional effects of PLM_{38-72} would not be masked by the presence of the γ-subunit, although this possibility cannot be ruled out.

2.3. NKA activity measurements

Enzymatic activities and protein contents were determined as described previously [26]. Here, assays of Na^{+}-activation of steady-state NKA activities (at 37 °C, pH 7.4, with 20 mM KCl, 3 mM ATP and 4 mM $MgCl_2$ in the assay medium) were performed by measuring phosphate liberation from ATP with colorimetric methods [27,28]. Inclusion of 1 mM ouabain served as a background control. The NKA concentration was 0.4 μg/ml and the concentration of PLM-peptide was 0.1 mM. The incubation with ATP lasted 15 min. PLM-peptides were solubilized in 10 mM histidine (pH 7.0) and kept at 20 °C for 120 min before use. The pH of the assay medium was not altered after the addition of any of the PLM peptides to 0.1 mM.

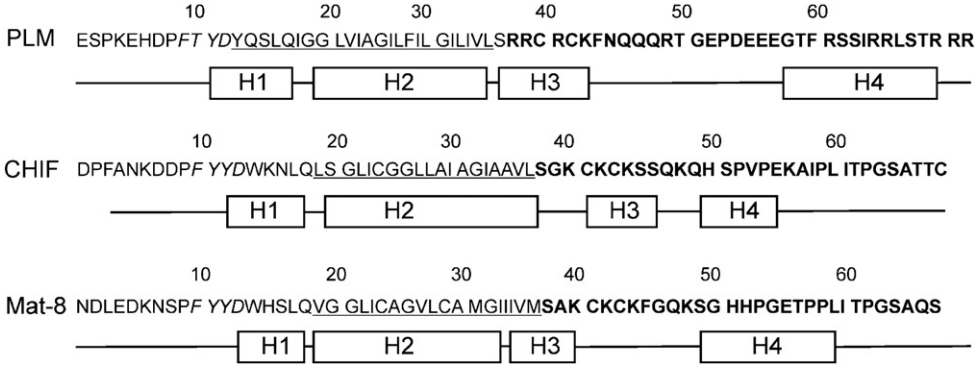

Fig. 1. Primary sequences of human PLM (FXYD1), Mat-8 (FXYD3) and CHIF (FXYD4). Highlighted are the FXYD sequence (italics), predicted transmembrane domain (underlined) and residues corresponding to the peptides studied here (bold). Below each sequence are secondary structure profiles showing the approximate length and position of helical regions (H1–H4) determined by solution-state NMR [20–22].

2.4. Nucleotide binding experiments

Equilibrium binding of nucleotides was measured in double-labeling filtration experiments essentially as previously described [29]. A 0.25 ml volume of a solution containing 0.2 mg/ml of NKA in buffer (30 mM NaCl, 10 mM histidine (pH 7.0) and 0.65 mM CDTA) with 0.05–45 μM [^{14}C]ADP, [^{3}H]glucose and 0 or 0.1 mM PLM was loaded on two stacked Millipore HAWP 0.45 μm filters; the enzyme remained adsorbed on the top filter, while the bottom one served as a control. The filters were separately counted in 4 ml Packard Filtercount scintillation fluid. The amount of nucleotide bound to the protein was calculated by subtracting from the total amount of nucleotide on the (top) filter (bound plus unbound nucleotide) the amount of unbound nucleotide, trapped in the filter together with the wetting fluid; the amount of unbound nucleotide was also proportional to the amount of [^{3}H]glucose in the same filter. Curve fitting for the nucleotide binding was performed using Origin 6.0 software (Microcal, Amherst, CA). Parameters derived are given with standard deviations.

2.5. Preparation of vesicles

Small unilamellar vesicles (SUVs) were prepared from DOPC alone or from binary DOPC/DOPS mixtures in 1:1, 2:1, 4:1 or 9:1 molar ratios. SUVs of 2:1 DMPC/DOPS and 2:1 DMPC/DOPG were also prepared. Lipids were prepared in chloroform and then dried under nitrogen and high vacuum, before resuspension in either 10 mM phosphate, pH 7, or 10 mM Tris, 1 mM EDTA, pH 7.4, with or without 30 mM NaCl. Sonication was carried out for 2–3 min on ice, using a Dawe Ultrasonic probe sonicator (London) at 50% duty cycle, output control 5, to promote formation of SUVs.

2.6. Isothermal titration calorimetry

Heat flow resulting from peptide binding to lipid vesicles was measured using the high-sensitivity standard VP-ITC or the ultrasensitive iTC$_{200}$ MicroCalorimeter (MicroCal LLC, Northampton, MA). Reaction cell volume and total injection volume were respectively, 1.4448 ml and 279.5 μl for the VP-ITC and 200 and 40 μl for the iTC$_{200}$. Experiments were performed at 25 °C, at a power reference setting of 15 μcal/s (VP-ITC), or 6 μcal/s (iTC$_{200}$) with stirring at 307 rpm (VP-ITC), or 1000 rpm (iTC$_{200}$). Prior to use all solutions were degassed under vacuum. Data analysis was carried out using the Origin v.7 software (MicroCal). Experimental conditions were designed following established protocols [30–32]. The reaction cell contained either a 50 μM (VP-ITC), or a 100 μM (iTC$_{200}$), solution of peptide (PLM$_{38-72}$ or pPLM$_{38-72}$), in 10 mM Tris; 1 mM EDTA, pH 7.4. A 10 mM suspension of lipid SUVs was prepared in the same buffer and injected via the syringe. Titrations were carried out at intervals up to 10 min in 10 μl (VP-ITC), or 0.5 and 1 μl (iTC$_{200}$), aliquots following an initial discard aliquot of 3 μl (VP-ITC), or 0.3 μl (iTC$_{200}$). Each injection generates a heat of reaction, determined by integration of the individual peaks from the heat flow trace. The heat of dilution was determined in controls experiments whereby lipid vesicles were titrated in to a buffer solution minus the peptide. Subtraction of the heat of dilution values from experimental values allows the determination of heat flow resulting from peptide binding to lipid.

2.7. Far UV circular dichroism

Secondary structural measurements of peptides were carried out on a Jasco J-180 spectropolarimeter. CD spectra were recorded from 250 to 195 nm using a 0.1 cm cuvette, a scan rate of 20 nm/min and an average of 4 accumulations per sample for trifluoroethanol (TFE) titrations and 8 accumulations for lipid titrations. All peptides were prepared to 50 μM in 10 mM phosphate, pH 7. Initial measurements were made using a stepwise titration with TFE to generate measurements up to 40% TFE. The experiment was then repeated titrating with SUVs of 50 mM DMPC/DOPG (2:1) resulting in lipid/peptide molar ratios of 50:1, 75:1, and 100:1. In each case controls were carried out by titrating TFE or SUVs into buffer minus the peptides and deducting the values obtained from the experimental values. The percentage α-helical content was calculated using the following equation [33]:

$$\%helix = 100 \times (\theta_{obs} - \theta_C) / (\theta_H - \theta_C) \quad (1)$$

where $\theta_H = -40000 \times (1 - x/n) + 100T$ and $\theta_C = 640 - 45T$. The quantities θ_H and θ_C represent the molar ellipticity values for 100% α-helix and 100% random coil, respectively, both expressed in deg. cm^2/dmol. The quantity θ_{obs} is the observed molar ellipticity measured at 222 nm, T is the temperature in °C, N is the number of amino acids, and x is a constant set at 2.5, which corrects for non-hydrogen bonded carbonyl groups.

2.8. NMR sample preparation

For solid-state NMR analysis of membrane-peptide interactions, 50 mg 2:1 DMPC/DOPG or 50 mg DOPC was dissolved in chloroform and dried to a film under nitrogen and high vacuum. The lipids were then resuspended in 50 μl of 10 mM phosphate with 1 mM EDTA at pH 7.4. Once NMR measurements had been carried out on the lipid control samples, peptide was added in 4 and 6 μl consecutive aliquots to give the desired final lipid to peptide molar ratio. Following addition of peptide, each sample was subject to 5 cycles of freeze/thawing and vortexed thoroughly before transferring to a 4 mm diameter zirconia MAS rotor or 5 mm sample tube.

2.9. Solid-state NMR measurements

Spectra were recorded on a Bruker Avance 400 MHz spectrometer operating at frequencies of 400.13 MHz for ^{1}H and 100.16 MHz for ^{13}C. All spectra were obtained with a Bruker variable temperature triple-resonance MAS probehead, with samples packed into a 4 mm diameter zirconium rotor. Cross-polarization magic-angle spinning (CP-MAS) ^{13}C SSNMR spectra were recorded at a sample rotation rate of 8 kHz. Hartmann-Hahn cross-polarization from ^{1}H to ^{13}C was achieved at a proton field of 66 kHz. Spectra were obtained by accumulating 50,000–70,000 transients with a 1.5-s recycle delay. Site-specific peptide-membrane interactions were monitored in a ^{13}C-observe, ^{31}P-dephase rotational-echo double-resonance (^{13}C(^{31}P) REDOR) SSNMR experiment [34] at a sample spinning rate of 5300 Hz. Two spectra were recorded. In the first, dipolar dephasing was achieved with a train of 8-μs 180° pulses at the ^{31}P frequency twice every sample rotation period (with xyxyyxyx phase cycling) and a single 8-μs 180° pulse at the ^{13}C frequency in the centre of the dephasing period to refocus isotropic ^{13}C chemical shifts. The total dephasing period was 5.4 ms. Continuous wave proton decoupling at 100 kHz was applied during the dephasing period and two-phase phase-modulated (TPPM) decoupling [35] at the same field was applied during acquisition. A second control ("full-echo") spectrum was obtained under identical conditions to the first, except that the ^{31}P dephasing pulses were omitted. Both spectra required the accumulation of 180,000 transients with a 1.5-s recycle delay, requiring a total experimental time of 6.25 days. The final spectra were the result of accumulating blocks of 20,000 transients, interleaved between control and dephased spectra to average the effects of drifts in tuning across both spectra. The REDOR spectra were collected at −30 °C and all other spectra were collected at 4 °C. The lower temperature was necessary for the REDOR measurements to eliminate molecular dynamics, which would otherwise average the weak ^{13}C-^{31}P dipolar couplings and attenuate dephasing. All spectra

were processed with the application of exponential multiplication (50 Hz line broadening) prior to Fourier transformation.

3. Results

3.1. Affinity of PLM peptides for phospholipid bilayers

ITC was used to monitor the thermodynamic parameters associated with the binding of PLM_{38-72} and $pPLM_{38-72}$ to vesicles of different phospholipid mixtures. The peptides were titrated with phospholipid SUVs until the peptide in the reaction cell was bound completely to the membranes and no further heat flow occurred. This procedure allows the total binding enthalpy ΔH_{tot} to be measured, from which a binding isotherm can be plotted and an apparent dissociation constant (K_D^{app}) calculated for the peptide [30–32,36,37]. First, experiments were carried out to compare the affinities of unphosphorylated PLM_{38-72} for membranes of zwitterionic DOPC and anionic DOPS bearing different surface charge, conferred by varying the proportions of the two lipids. Raw enthalpic data for DOPC/DOPS injections into PLM_{38-72} at an ionic strength of 30 mM NaCl indicated that the lipid–peptide interaction is exothermic (data not shown). Corresponding plots of enthalpy changes (ΔH_k) per mole of peptide, expressed as a function of lipid/peptide molar ratio (i.e., for each injection k of lipid into the cell), are shown for SUVs of different DOPC/DOPS composition in Fig. 2a to e. The total binding enthalpy ($\Delta H_{tot} = \sum \Delta H_k$) for the peptide increases with membrane surface charge, from virtually zero for pure DOPC to 723 kcal/mol for 1:1 DOPC/DOPS (Fig. 2f). In parallel, fewer lipid injections are required to achieve saturation of the membranes by the peptide. A semi-quantitative measure of affinity is obtained by transforming the calorimetric data into a binding isotherm expressing the molar ratio of membrane-bound peptide per lipid (X_b) as a function of the

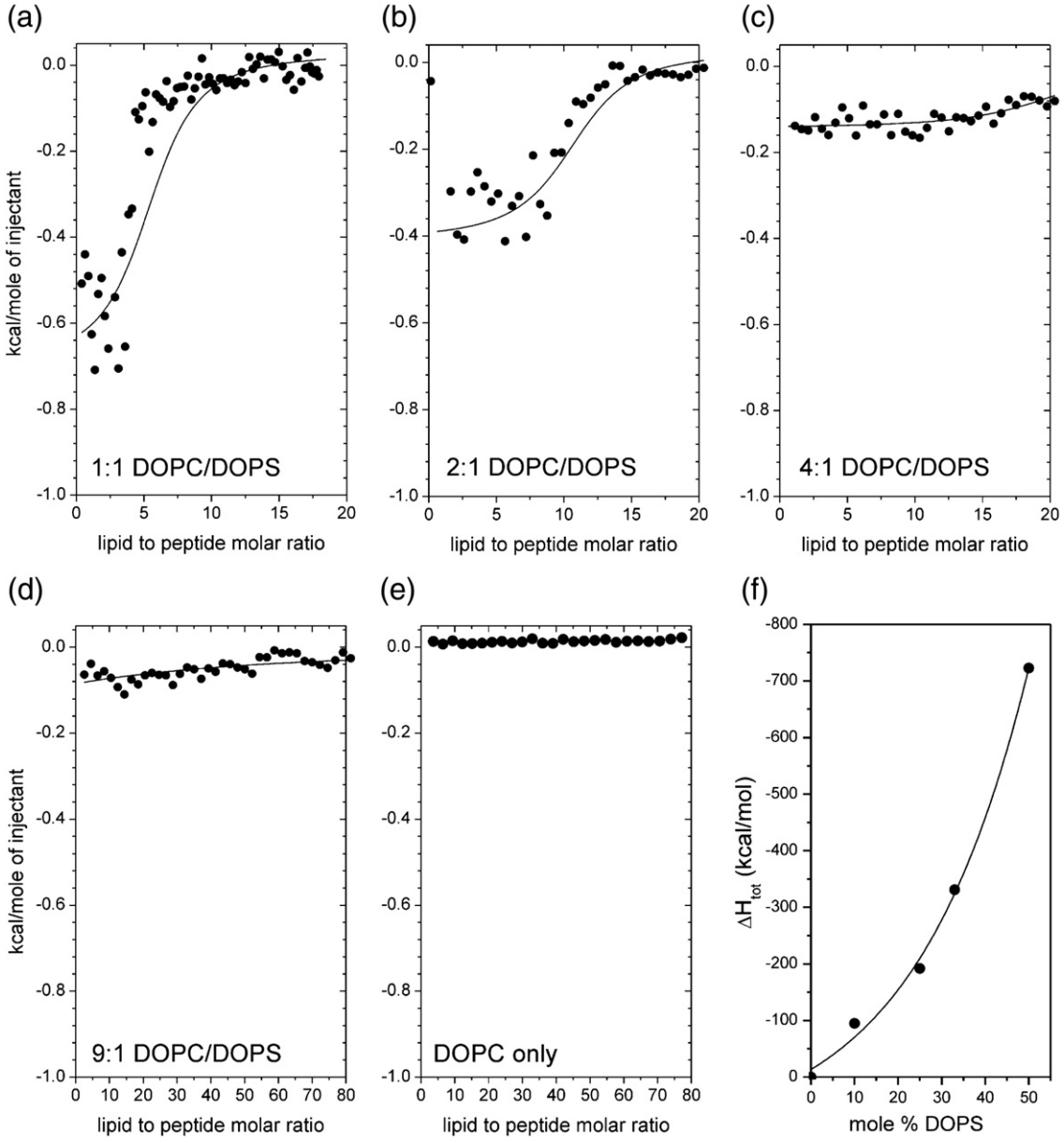

Fig. 2. ITC measurements of PLM_{38-72} interactions with phospholipid membranes of different surface charge. Heat flows are shown for 100 μM PLM_{38-72} titrated with lipid vesicles (25 to 50 μM lipid per injection) composed of DOPC and DOPS in molar ratios of 1:1 (a), 2:1 (b), 4:1 (c), 9:1 (d) and for DOPC alone (e). Curves were generated by integrating the raw enthalpic data following subtraction of the heat of dilution for the peptide. The data were fitted by the MicroCal 'one set of sites' function (black lines). Total binding enthalpy (ΔH_{tot}) for PLM_{38-72} is plotted as a function of DOPC/DOPS membrane surface charge (f).

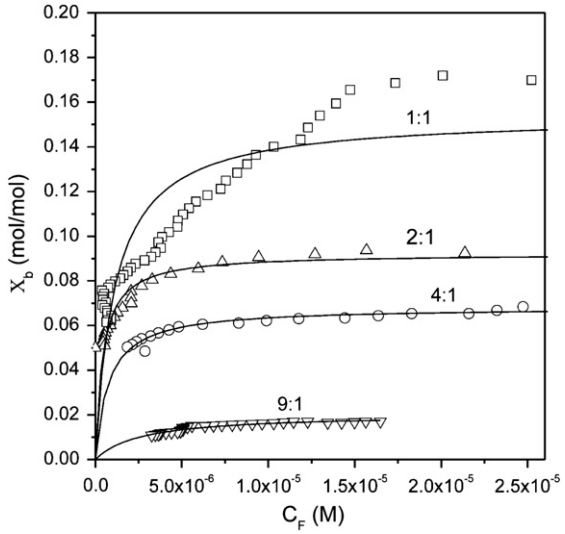

Fig. 3. Affinity of PLM_{38-72} for DOPC/DOPS membranes bearing different surface charge. ITC binding isotherms are shown for PLM_{38-72} titrated with 1:1 DOPC/DOPS (squares), 2:1 DOPC/DOPS (up triangles), 4:1 DOPC/DOPS (circles) and 9:1 DOPC/DOPS (down triangles). Solid lines represent the best fits to the data obtained with Eq. (2).

equilibrium (molar) concentration of free peptide in bulk solution (C_F) [32,38–40]. By assuming a simple single-site binding model an apparent dissociation constant (K_D^{app}) can be estimated with the equation:

$$X_b = \frac{X_b^{sat}.C_F}{C_F + K_D^{app}} \quad (2)$$

A more rigorous analysis of peptide-membrane interactions requires knowledge of the membrane surface potential, which can be estimated from the surface charge density using Gouy-Chapman theory [38]. The more simple approach in Eq. (2) is sufficient to observe trends in the relative affinity of a single peptide for different membranes, or to compare the affinities of phosphorylated and non-phosphorylated variants of the same peptide for the same lipid systems [38]. Binding isotherms for PLM_{38-72} titrated with different DOPC/DOPS membranes are shown in Fig. 3 and Table 1 summarizes the values of K_D^{app} and the binding capacity (expressed as the moles of peptide bound per mole of lipid at saturation). The membrane affinity of PLM_{38-72} decreases by almost two orders of magnitude when the negative surface charge is reduced from 33% (i.e. 2:1 DOPC/DOPS) to 10% (i.e., 9:1 DOPC/DOPS), and the binding capacity is also reduced substantially. The 9:1 DOPC/DOPS is representative of eukaryotic cells, in which the cytoplasmic leaflet of the plasma membrane contains approximately 10–15% anionic lipids. For instance, microsomes from kidney outer medulla contain approximately 8% phosphatidylserine and 7% phosphatidylinositol as the major anionic lipids [41]. Interestingly, the isotherm for 1:1 DOPC/DOPS and, to a lesser degree, the isotherm for 2:1 DOPC/DOPS, deviate from the best fitting curve generated with Eq. (2) (Figs. 2a, b and 3). The origin of this non-ideal behavior is not known at this stage, but an alternative analytical model will be required to interpret these binding isotherms more accurately. One possible explanation is that the peptide induces lateral phase separation of the zwitterionic and anionic lipids at high DOPS concentrations. Previous ^2H wide-line and ^{31}P MAS NMR measurements of PLM_{37-72} interactions with 2:1 DMPC/DOPG membranes were consistent with such a phenomenon [23].

The effect of phosphorylation at S68 on the membrane affinity of PLM_{38-72} was investigated by ITC experiments in which peptides were titrated with membranes bearing the same negative surface charge (33%) but differing in the hydrocarbon chain content (C18 unsaturated dioleoyl or C14 saturated dimyristoyl) and/or in the chemical nature of the anionic headgroup (serine or glycerol). Fig. 4 shows binding isotherms for PLM_{38-72} and $pPLM_{38-72}$ titrated with 2:1 DOPC/DOPS, 2:1 DMPC/DOPS and 2:1 DMPC/DOPG. Although the two peptides had different affinities for the three membrane systems, in each case phosphorylation resulted in a large reduction in the affinity for the membranes (Table 1). Titration of the phosphorylated peptide with the physiologically representative 9:1 DOPC/DOPS membranes resulted in no detectable heat flow (data not presented), indicating that membrane interactions did not occur or were very weak.

CD spectroscopic measurements on PLM_{38-72} and $pPLM_{38-72}$ (Fig. 5a and b, open circles) indicate that both peptides are essentially unfolded in pure aqueous solution. CD spectra of PLM_{38-72} titrated with 2:1 DOPC/DOPS, 2:1 DMPC/DOPS or 2:1 DMPC/DOPG vesicles (at a lipid/peptide molar ratio of 75:1) are consistent in each case with an increase in the helical content of the peptide (Fig. 5a and Table 2). The membrane surface appears to stabilize the peptide in an amphipathic helix, as reported elsewhere [19,21–23], although in each case the estimated helical content is less than 10% (Table 2). By comparison, the peptide is approximately 13% α-helix after titration of the solution with 40% trifluoroethanol (TFE), which promotes intramolecular hydrogen bonding and favors α-helical formation where an intrinsic propensity for it exists. Interestingly, the DMPC/DOPS membranes appear to induce a higher proportion of α-helix in PLM_{38-72} than do the other membranes, suggesting that the peptide is sensitive to the chemical structure of the lipid head-groups and the acyl chains. By contrast, $pPLM_{38-72}$ remains essentially unfolded in the presence of the same membrane systems and TFE under identical conditions (Fig. 5b and Table 2). The phosphorylated peptide thus has a lower propensity to form a helix in the presence of a saturating concentration of vesicles.

3.2. Affinity of Mat-8 and CHIF peptides for phospholipid bilayers

Experiments were undertaken to measure the membrane affinity of peptides derived from the cytoplasmic domains of Mat-8 ($Mat\text{-}8_{38-67}$)

Table 1
Summary of binding capacity (X_b^{sat}, expressed as mole peptide per mole lipid) and apparent dissociation constant (K_D^{app}) from ITC measurements of phospholipid membranes titrated with PLM_{38-72} and $pPLM_{38-72}$. A correction factor of 0.6 was applied in the calculations, since not all the lipid surface is available to the peptide for binding [32].

Membrane	PLM_{38-72}		$pPLM_{38-72}$	
	X_b^{sat} (mol/mol)	K_D^{app} (M^{-1})	X_b^{sat} (mol/mol)	K_D^{app} (M^{-1})
1:1 DOPC/DOPS[a]	0.153	–	Not measured	
2:1 DOPC/DOPS[b]	0.092 (0.011)	$7.51\ (2.30)\times10^{7}$	0.111 (0.073)	$1.83\ (0.77)\times10^{-5}$
4:1 DOPC/DOPS	0.068	9.18×10^{-6}	Not measured	
9:1 DOPC/DOPS	0.020	8.11×10^{-5}	Not measured	
DOPC	Enthalpy changes are below level of detection			
2:1 DMPC/DOPS[b]	0.136 (0.053)	$3.67\ (2.13)\times10^{-6}$	0.102 (0.037)	$1.63\ (0.64)\times10^{-5}$
2:1 DMPC/DOPG[b]	0.232 (0.049)	$3.07\ (1.79)\times10^{-6}$	0.282 (0.033)	$1.56\ (0.20)\times10^{-5}$

[a] Binding isotherm does not conform to ideal Eq. (2). X_b^{sat} is therefore an approximate value and K_D^{app} was not determined.
[b] Isotherms measured in triplicate. Mean values are given with standard deviations in parentheses.

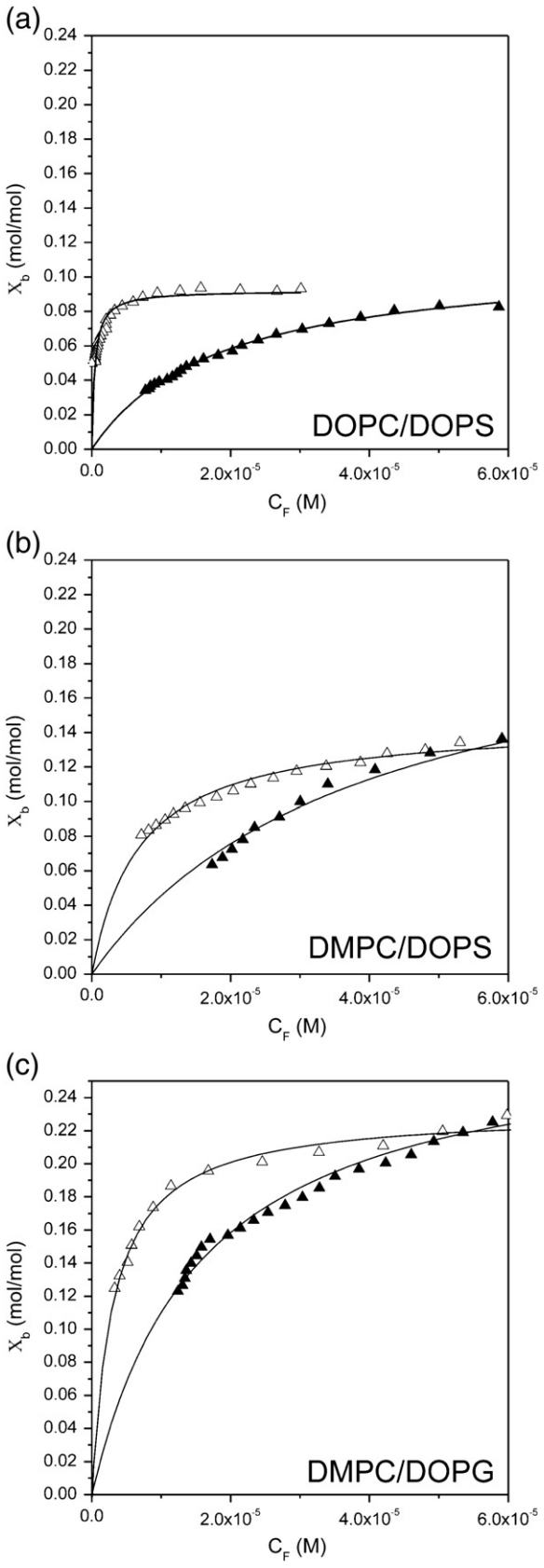

Fig. 4. Effect of PLM_{38-72} phosphorylation on membrane affinity. ITC binding isotherms are shown for PLM_{38-72} (open triangles) or $pPLM_{38-72}$ (filled triangles) titrated with 2:1 DOPC/DOPS (a), 2:1 DMPC/DOPS (b) or 2:1 DMPC/DOPG (c). Solid lines represent the best fits to the data obtained with Eq. (2).

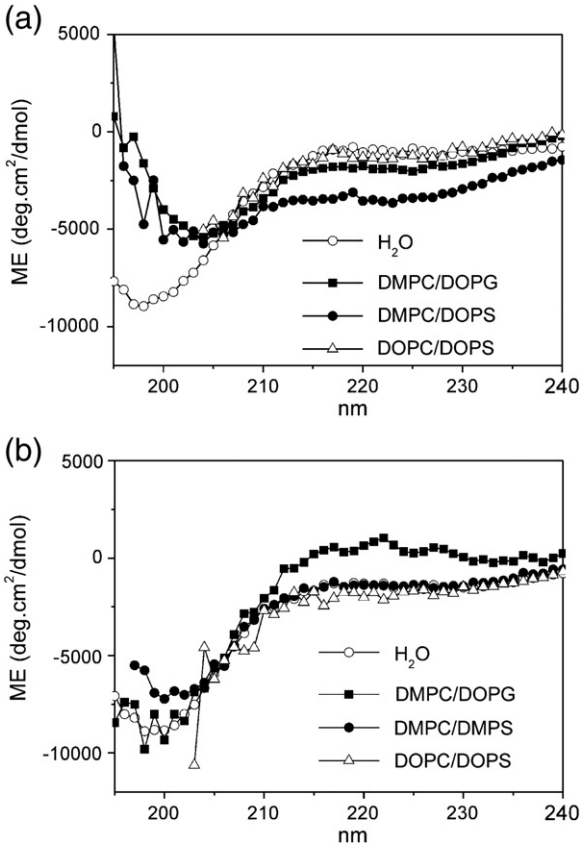

Fig. 5. Far UV CD measurements of PLM peptide secondary structure. Spectra are shown for 50 μM PLM_{38-72} (a) and $pPLM_{38-72}$ (b) in 10 mM phosphate, pH 7, alone (open circles) or in the presence of 2:1 DMPC/DOPG vesicles (filled squares), 2:1 DMPC/DOPS (filled circles) or 2:1 DOPC/DOPS (triangles) at a 75:1 lipid/peptide molar ratio. Note that the signal for the DOPC/DOPS sample has been truncated below 205 nm because these lipids gave rise to scattering effects at lower wavelengths.

and CHIF ($CHIF_{38-69}$). The cytoplasmic domains of Mat-8 and CHIF lack the arginine-rich sequence of PLM (Fig. 1). ITC measurements were performed on the peptides titrated with either DOPC or 2:1 DMPC/DOPG vesicles. No heat flow was detected when $CHIF_{38-69}$ was titrated with either of these vesicles, indicating that no binding occurred or else that the interaction was too weak to observe (data not presented). Similarly no heat flow was detected in the titration of Mat-8_{38-67} with DOPC, but a small endothermic reaction occurred for Mat-8_{38-67} titrated with DMPC/DOPG (Fig. 6a). Analysis of the binding isotherm indicated that the binding was very weak, with K_D^{app} in the millimolar range, although the errors were rather large owing to the small endothermic response. CD analysis indicated that Mat-8_{38-67} is unstructured in aqueous solution and only minor structural changes occur in the presence of DMPC/DOPG membranes (Fig. 6b). The Mat-8 and CHIF cytoplasmic domains thus have substantially lower membrane affinities than the PLM cytoplasmic domain. The NMR-determined structure of CHIF incorporated into oriented lipid bilayers of 4:1 DOPC/DOPG places

Table 2
Estimates of percentage α-helix for PLM_{38-72} and $pPLM_{38-72}$ calculated from CD molar ellipticity values measured at 222 nm according to Eq. (1). Spectra were measured in the presence of 40% TFE or lipid SUVs at a 75:1 lipid/peptide molar ratio.

	PLM_{38-72}	$pPLM_{38-72}$
Water	3.8	1.7
TFE	13.4	3.3
2:1 DMPC/DOPG	6.4	2.4
2:1 DMPC/DOPS	8.9	2.7
2:1 DOPC/DOPS	2.7	2.8

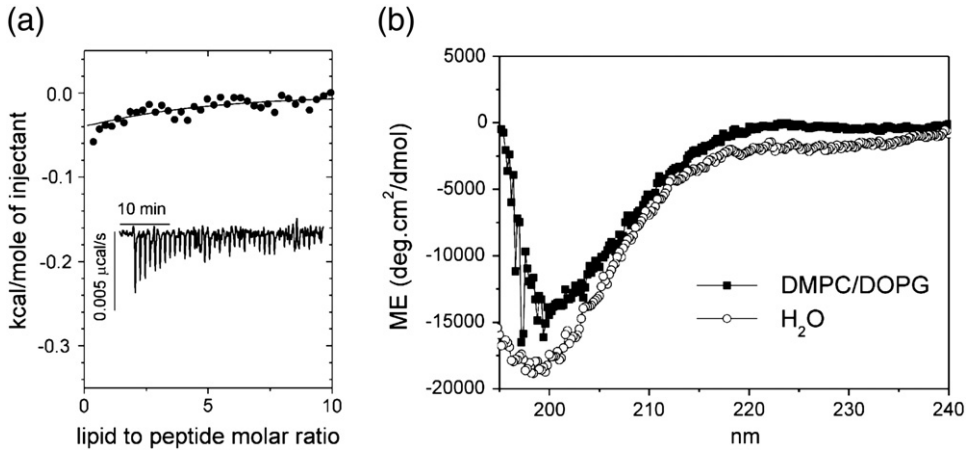

Fig. 6. Measurements of Mat-8_{38-67} interactions with 2:1 DMPC/DOPG membranes. (a) ITC heat flows for 100 µM Mat-8_{38-67} titrated with lipid vesicles (25 to 50 µM lipid per injection). The inset shows the raw enthalpic data. (b) Far UV CD measurements of 50 µM Mat-8_{38-67} in 10 mM phosphate, pH 7, alone (open circles) or in the presence of 2:1 DMPC/DOPC vesicles (filled squares) at a 75:1 lipid/peptide molar ratio.

cytoplasmic helix H4 (Fig. 1) at an orientation of 60°–80° relative to an axis perpendicular to the membrane surface [42,43]. This model, viewed in the light of our results, implies that the CHIF cytoplasmic domain lies close to the surface of the membrane but is not in contact with the lipid headgroups.

3.3. SSNMR measurements of PLM_{38-72}–membrane interactions

CP-MAS NMR can provide detailed information about the nature of peptide-membrane interactions if signals are observed from ^{13}C labels placed at strategic sites in the peptide. Here, a spectrum of 2:1 DMPC/DOPG membranes with [^{13}C,^{15}N]PLM_{38-72} at 30 °C displays a signature peak from the arginine guanidinium groups of the peptide at 156.6 ppm, which is distinct from the background peaks from the lipids (Fig. 7a, top) and present in the solution spectrum of the peptide (Fig. 7a, bottom) but absent from the CP-MAS spectrum of lipid only. The presence of this peak confirms that the peptide associates with the negatively charged membranes and that the cationic arginine side groups are motionally restrained. Fig. 7b (top) shows that the guanidinium peak intensity reaches a maximum at a contact time of around 6 ms, which is expected for a nonprotonated carbon in a restrained environment [44]. By contrast, no signals can be seen for [^{13}C,^{15}N]PLM_{38-72} in the presence of 2:1 DMPC/DOPC membranes under identical conditions (Fig. 7b, bottom) indicating that the arginine groups are not restrained by the zwitterionic lipids.

Further SSNMR experiments investigated whether PLM_{38-72} is able to interact with the lipids of a native kidney membrane preparation containing NKA and other integral membrane proteins. The composition of kidney membranes is approximately 0.87 mg phospholipid per mg protein [45], of which ~19% are anionic [41], and the method described in Fig. 7 is unsuitable because it cannot distinguish between peptide–lipid and peptide–protein interactions. Instead, $^{13}C(^{31}P)$-REDOR SSNMR was used to determine whether the cationic arginine residues of [^{13}C]PLM_{38-72} lie close to the negatively charged phosphate group of the lipids in frozen kidney membranes (see Refs [46,47] for recent examples of similar experiments). Fig. 8a shows a control full-echo $^{13}C(^{31}P)$-REDOR difference spectrum of [^{13}C]PLM_{38-72} in kidney membranes at an approximately 20:1 lipid/peptide molar ratio. A difference spectrum (Δ), obtained by subtracting a dephased spectrum from the control, highlights dephasing of the guanidinium signal at 156.6 ppm, indicating that one or more of these groups must be situated close to the lipid phosphate groups. It is not possible to determine accurate peptide–lipid distances from these data, but calculations based on an isolated ^{31}P-^{13}C spin pair predict that one or more of the labeled arginine groups lie within ~6 Å of the membrane surface to give rise to detectable dephasing under the conditions of this experiment. Additional experiments at longer dephasing times were not attempted because the limited sample size, unfavorable relaxation and poor sensitivity

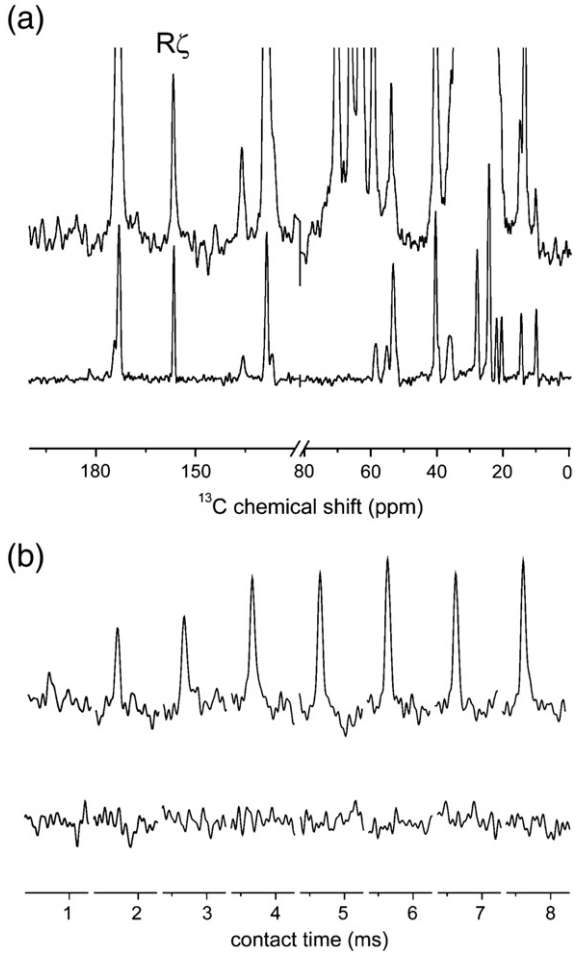

Fig. 7. ^{13}C SSNMR experiments (at 4 °C) to detect interactions between PLM_{38-72} and phospholipid membranes. (a) A ^{13}C CP-MAS SSNMR spectrum of 2:1 DMPC/DOPG membranes containing [^{13}C]PLM_{38-72} at a 20:1 lipid/peptide molar ratio (top) and a ^{13}C NMR spectrum (with direct polarization) of [^{13}C]PLM_{38-72} alone in phosphate buffer (bottom). The peak at 156.6 ppm is characteristic for the guanidinium carbons (Cζ) of arginines R61, R65, R66 and R67 is labeled Rζ. (b) ^{13}C peak intensities for Rζ in CP-MAS SSNMR spectra of [^{13}C]PLM_{38-72} in 2:1 DMPC/DOPG membranes (top) and 2:1 DMPC/DOPC membranes (bottom) at the variable contact times shown.

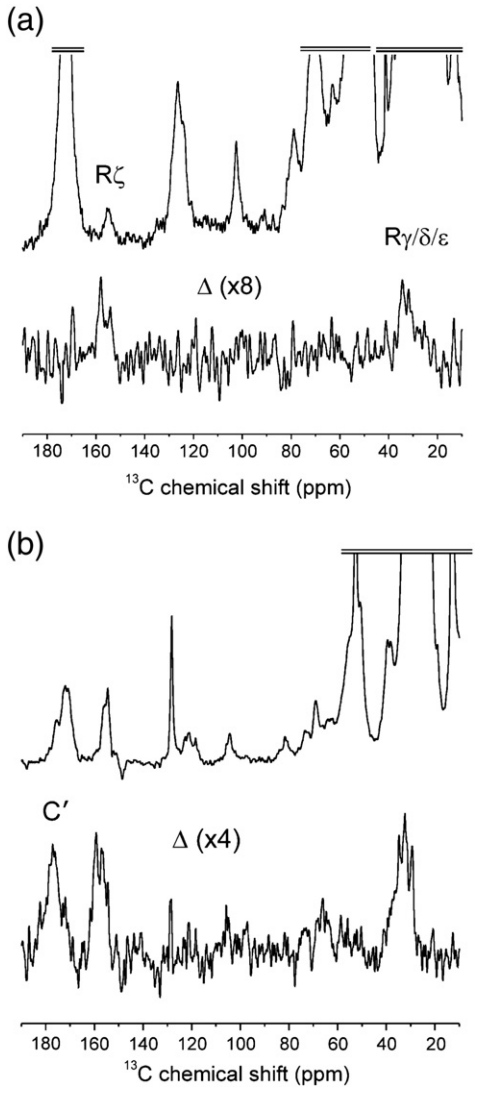

Fig. 8. ^{13}C[^{31}P]-REDOR SSNMR experiments (at −30 °C) to detect interactions between PLM_{38-72} and phospholipids in kidney membranes. (a) Spectra of kidney membranes with PLM_{38-72} at a lipid/peptide molar ratio of approximately 20:1. The full-echo spectrum is shown above the difference spectrum (Δ) obtained as described in the Experimental section. (b) Full-echo (top) and difference (bottom) ^{13}C[^{31}P]-REDOR spectra of 2:1 DMPC/DOPG membranes with PLM_{38-72} at a 20:1 lipid/peptide molar ratio. The difference spectra are expanded vertically either 4-fold (×4) or 8-fold (×8).

required impractically long acquisition times. A repeat of the experiment for [^{13}C]PLM_{38-72} in DMPC/DOPG membranes showed much stronger dephasing of the arginine guanidinium signal at ~160 ppm and also signals corresponding to side group carbons (Rβ/γ/δ) at ~30 ppm and to carbonyl carbons (C′) at ~170 ppm (Fig. 8b). This experiment thus indicates that the peptide can interact with phospholipid headgroups in the presence of NKA, but either the contact is less intimate or a smaller fraction of the peptide is associated with the headgroups compared with the pure lipid membranes.

3.4. Regulation of NKA by FXYD peptides

The sodium-dependence of the ATPase activity was measured in presence of PLM_{38-72} and $pPLM_{38-72}$ at a peptide concentration of 100 μM, and in the absence of peptide. Residues 38–72 of full length PLM are confined within a hemispherical space at the surface of the two-dimensional lipid matrix and thus the local concentration exposed to NKA is high. A high concentration of PLM_{38-72} was therefore chosen to compensate for the free diffusion of the soluble peptide in the large relative volume of the aqueous phase [48].

Fig. 9a shows the sodium-dependence of the ATPase activity in the presence of 20 mM KCl. Control enzyme is half-maximally activated by $K_{0.5} = 13.5$ mM NaCl, with maximal activity (V_{max}) obtained at about 100 mM NaCl (see also Table 3). The activity data, which represent one of three experiments on freshly prepared enzyme and peptide samples, are analyzed using a Hill equation:

$$V = V_{max} \cdot \left[Na^+\right]^n / \left(K_{0.5}{}^n + \left[Na^+\right]^n\right) \quad (3)$$

from which the kinetic parameters V_{max}, $K_{0.5}$ and the Hill coefficient n are obtained from non-linear least squares fitting of the data (summarized in Table 3). PLM_{38-72} decreases V_{max} to 59 ± 10% of the control ($p<0.05$), and $K_{0.5}$ for Na^+ is increased to about 16 mM. $pPLM_{38-72}$ also reduces V_{max} (to 79 + 3.9% of the control) but inhibition of maximal activity is significantly lower than is observed for PLM_{38-72} ($p<0.05$). Interestingly, $pPLM_{38-72}$ also increases $K_{0.5}$ to 16 mM, implying that phosphorylation of the peptide partially relieves inhibition of maximal enzyme activity but does not recover the lowered sodium affinity of NKA. The shorter peptide PLM_{63-72} has no effect on V_{max} and only leads to a small increase in $K_{0.5}$ for Na^+,

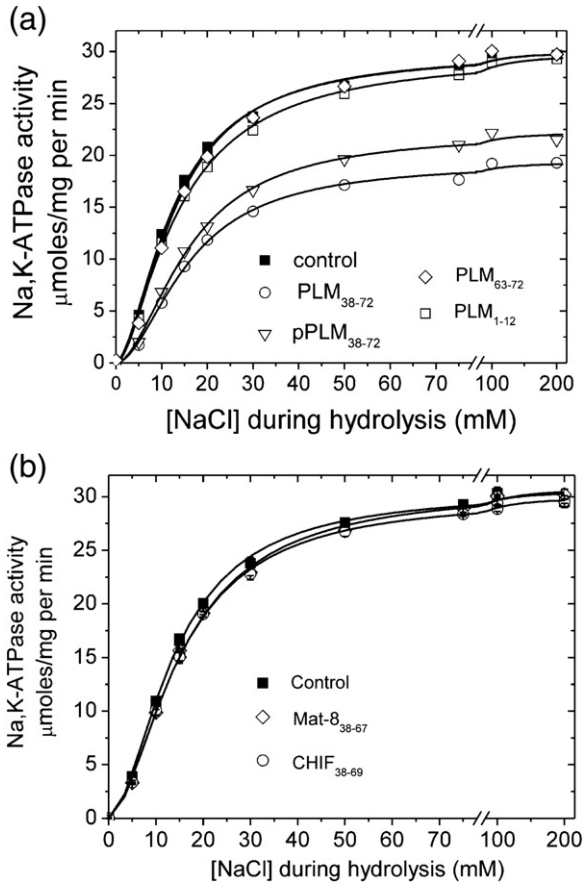

Fig. 9. Effects of PLM peptides on ATP hydrolysis by NKA in kidney membrane preparations. (a) Activation of ATP hydrolysis by Na^+ in the presence of PLM peptides. Kidney NKA activity was determined at the indicated concentrations of Na^+ in the presence of 20 mM KCl, 3 mM ATP, 4 mM $MgCl_2$ (pH 7.4 at 37 °C) and 100 μM peptide. Control NKA (absence of peptide), filled squares; PLM_{63-72}, open diamonds; PLM_{1-12} open squares; $pPLM_{38-72}$, open down-triangle; PLM_{38-72}, open circles. The full lines represent non-linear least-squares fits to a Hill equation with the parameters for V_{max}, $K_{0.5}$ and Hill coefficient n shown in Table 3. Mean values from 3 measurements are shown at each Na^+ concentration. Error bars are included but do not extend beyond the symbols and are not visible. (b) Activation of ATP hydrolysis by Na^+ in the presence of 100 μM $Mat\text{-}8_{38-67}$ (diamonds) or 100 μM $CHIF_{38-69}$ (circles).

Table 3
Activation of NKA hydrolysis by Na^+ in the presence of peptides derived from PLM. Data in Fig. 9 were fitted by a Hill-type equation (see text) and parameters for maximal hydrolytic activity (V_{max}, expressed as micromoles ATP hydrolyzed/mg per min at 37 °C) as well as the half-maximal activating concentration of Na^+ ($K_{0.5}$, expressed as mM Na^+) in the presence of 20 mM KCl were extracted. The sigmoidicity of the activation curve is described by the Hill-coefficient (n). Mean values for V_{max} and $K_{0.5}$ are calculated from 9 measurements for control, PLM_{38-72} and $pPLM_{38-72}$ groups and 3 measurements for PLM_{1-12} and PLM_{63-72} groups. Standard errors are given in brackets.

Parameter	Treatment				
	Control	PLM_{38-72}	$pPLM_{38-72}$	PLM_{1-12}	PLM_{63-72}
V_{max}	30.0 (1.8)	17.7 (3.0)	23.7 (1.2)	29.9 (2.1)	29.7 (2.1)
$K_{0.5}$	13.5 (0.41)	15.9 (0.47)	16.0 (0.46)	14.0 (0.41)	14.2 (0.41)
n	1.7	1.8	1.8	1.6	1.7
χ^2	24.8	9.6	11.7	15.9	25.3
R^2 (×100)	99.8	99.8	99.8	99.9	99.5

indicating that some or all of the residues 38–62 are required directly for the inhibitory effect, or else are needed to stabilize the 10 C-terminal residues in an inhibitory conformation. NKA activity is also unaffected by the peptide PLM_{1-12} representing the extracellular region containing the FXYD motif. Mat-8 and CHIF had no effect on NKA activity at a 100 μM peptide concentration (Fig. 9b).

Fig. 10 shows the effect of PLM_{38-72} and $pPLM_{38-72}$ on ADP binding to NKA. In the presence of about 30 mM NaCl the dissociation constant for ADP is about 0.4 μM (±0.04) for control NKA, and addition of 0.1 mM PLM_{38-72} or $pPLM_{38-72}$ leads to a slightly weaker binding of ADP (Fig. 10a and b). It is notable that the two peptides induce additional binding of ADP, which is completely absent in control enzyme (compare circles and squares in Fig. 10). The high affinity binding of ADP to NKA (E) is described by the classical scheme

$$E + A \Leftrightarrow EA$$

characterized by the equilibrium constant

$$K_d = \frac{[E]\cdot[A]}{[EA]}. \quad (4)$$

The binding curve for control enzyme was fitted by the single hyperbolic function:

$$[EA] = \frac{[EA]_{max}\cdot[A]}{K_d + [A]} \quad (5)$$

The nucleotide binding capacity is about 2.8 nmol/mg protein with equilibrium dissociation constant K_d for ADP of about 0.4 μM as found before [29]. In the presence of PLM_{38-72} or $pPLM_{38-72}$ the additional component seen at the higher concentrations of ADP appears to be a linear function of the ADP concentration (defined by constant K_{add}), and the data are fitted adequately by a function

$$[EA] = \frac{[EA]_{max}\cdot[A]}{K_d + [A]} + K_{add}\bullet[A] \quad (6)$$

Non-linear least squares fitting of this function to both sets of data (keeping $[EA]_{max} = 2.8$ nmol/mg protein) shows that both peptides increase the dissociation constant for ADP to about 0.7 μM (±0.10) with an additional non-specific binding-capacity of about $K_{add} = 0.084$ nmol ADP/mg protein per μM ADP (±0.002). The additional component does not show signs of saturation at the concentrations of ADP used here (up to 45 μM) and can either be due to unmasked additional sites on NKA or to interactions with PLM, which itself is adsorbed to the NKA-membranes (and thus retained on the filters). This second explanation is supported in part by ITC measurements of a 100 μM PLM_{38-72} solution titrated with ADP (not presented), which showed that the nucleotide binds to peptide in a 1:1 stoichiometry with a dissociation constant of 7.8 μM and reaching saturation at approximately 160 μM ADP. The physiological relevance of this interaction is unknown and is not investigated further here.

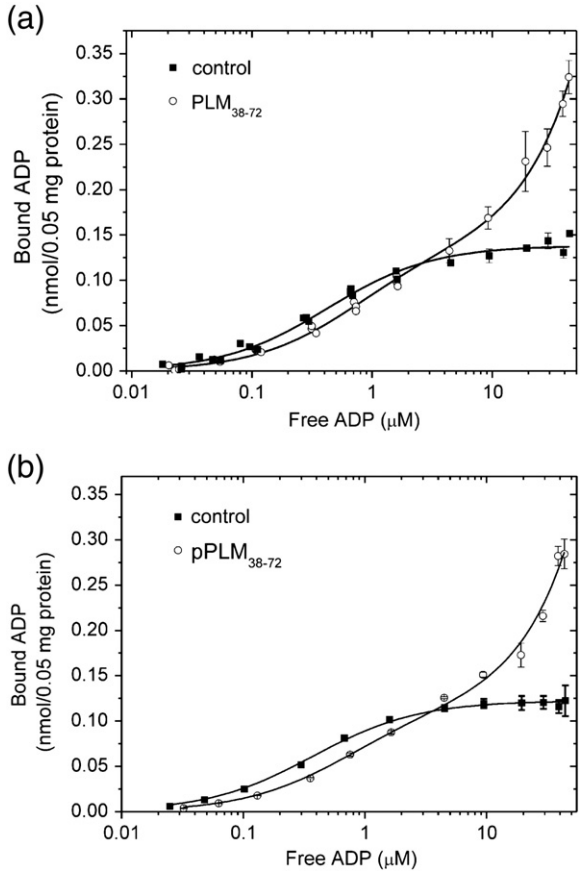

Fig. 10. Effects of PLM peptides on nucleotide binding by NKA in kidney membrane preparations. (a) Equilibrium binding of [^{14}C]ADP to NKA in the presence of 100 μM PLM_{38-72} (open circles) and in the absence of PLM_{38-72} (filled squares). Each filter contains 0.05 mg protein. The full line through the control data (filled squares) represent a single hyperbolic function with maximal binding capacities of about 0.14 nmol/0.05 mg protein and a dissociation constant for ADP of 0.43 μM (±0.04, $n = 3$). The full line through the PLM-data (open circles) represents a single hyperbolic function with a dissociation constant for ADP of 0.73 μM (±0.09, $n = 3$) together with a linear component with a slope of 0.0042 (±0.0001, $n = 3$) nmol ADP bound/0.05 mg protein per μM ADP (see text). The maximal binding capacities for the specific binding in this fitting procedure was fixed to the same as for control enzyme, 0.14 nmol/0.05 mg protein. (b) Equilibrium binding of [^{14}C]ADP to NKA in the presence of 100 μM $pPLM_{38-72}$ (open circles) and in the absence of $pPLM_{38-72}$ (filled squares). The dissociation constant for ADP is 0.70 μM (±0.19). Conditions are as in (a) but using 0.048 mg protein.

4. Discussion

4.1. Functional role of the PLM cytoplasmic domain

Several studies have demonstrated that PLM contributes to the maintenance of normal cardiac function through the functional modulation of NCX1 and NKA [4,15,49–53], although there is debate as to whether PLM increases or reduces the ionic affinity and maximal activity of NKA [54,55]. In the heart, NKA is the primary mechanism of Na^+ extrusion, and a decrease in cardiac NKA activity post-myocardial infarction and in heart failure [56–58] has been linked to PLM overexpression and a down-regulation of NKA expression [57]. The pathophysiological consequences of alterations in PLM expression may be offset by the elevation of PLM phosphorylation [58] and/or phosphatase activity [59]. The cytoplasmic domain of PLM alone reduced ouabain-sensitive sodium currents in PLM-depleted myocytes and

NKA was stimulated by treatment of cells with PLM_{54-72} phosphorylated at S68 [15]. The nature of the NKA-PLM interaction in lipid bilayers is unclear, and current models are based upon NMR structural analysis of PLM alone in SDS micelles. In these models the cytoplasmic domain aligns parallel with the membrane surface and thus interacts with NKA at the interface with the lipid headgroups [20]. These latter observations provide an incentive to study in more detail the cytoplasmic C-terminal region of PLM, focusing on how phosphorylation modulates its interactions with lipid membranes and with NKA.

4.2. Membrane interactions of the PLM cytoplasmic domain

With the peptide PLM_{38-72} the membrane surface interactions of the PLM cytoplasmic domain were investigated in isolation from the remainder of the protein. The C-terminal region of PLM_{38-72} is rich in arginine residues and is thus highly basic, and our earlier work showed that the peptide binds as an amphipathic helix to anionic phospholipid surfaces [23]. Here, ITC experiments provide a more quantitative measure of the membrane affinity of PLM_{38-72} before and after phosphorylation. As expected, the peptide has the highest affinity for the most negatively charged membranes (i.e., consisting of over 50% anionic phospholipids). This agrees with the NMR structural model of PLM in anionic SDS micelles, in which the cytoplasmic domain aligns along the charged micelle surface. The membrane affinity of PLM_{38-72} is reduced substantially after phosphorylation at S68. This contrasts with NMR studies of full-length PLM in SDS micelles, which indicate that phosphorylation does not alter significantly the position of the cytoplasmic domain at the membrane surface. In the latter case, the transmembrane domain of PLM may help to anchor the cytoplasmic domain to the membrane surface. Importantly, PLM_{38-72} has a substantially weaker interaction with membranes carrying ~10% anionic phospholipids, which is more representative of the native membrane environment. The physiological effect of phosphorylation on an already weak membrane interaction may therefore be insignificant. Furthermore, although the membrane affinities of the Mat-8 and CHIF cytoplasmic domains are much lower than seen for PLM_{38-72} in our model systems, this distinction may be less pronounced in the native membrane environments if the membrane affinity of PLM_{38-72} is also low.

4.3. Effect of FXYD cytoplasmic peptides on NKA function

PLM_{38-72} regulates NKA activity in a membrane preparation from kidney, by lowering slightly the affinity of the enzyme for sodium and depressing (by ~30%) the maximal ATPase activity at saturating sodium concentrations (Fig. 9). The reduced affinity of NKA for nucleotide in the presence of the peptide (Fig. 10) suggests that there may be some overlap in the peptide and nucleotide binding sites on the cytoplasmic face of the enzyme. This interpretation should be treated with caution, however, because a decrease in K_d for ADP could also occur if PLM acts as K^+ (inducing the E2-form). From the activity data we also see a requirement for more Na^+ for activity, which in a simplified analysis means the same thing, namely that PLM pushes NKA towards the E2-form. Phosphorylation of PLM_{38-72} at S68 partially (but statistically significantly) reverses the effect of the peptide on V_{max} but does not alleviate the lower affinity for sodium. The effect of the peptides on sodium affinity parallels the nucleotide affinity of NKA, which is reduced by a similar amount by both PLM_{38-72} and $pPLM_{38-72}$. That phosphorylation of PLM_{38-72} affects V_{max} but not the sodium or nucleotide affinity of NKA suggests that the peptide affects one or more stages of the catalytic cycle of NKA following binding of sodium or ATP.

Interestingly, $Mat\text{-}8_{38-67}$ and $CHIF_{38-69}$ do not have any appreciable effect on NKA activity, suggesting that the cytoplasmic domains of Mat-8 and CHIF have quite different functional characteristics to those of PLM. We speculate that one explanation for this distinction is that PLM is a known phosphorylation substrate whereas Mat-8 and CHIF are not. Phosphorylation may therefore serve as a functional switch in the PLM cytoplasmic domain, but Mat-8 and CHIF have evolved functionally inert cytoplasmic domains for which phosphorylation would be redundant.

5. Conclusions

This work has found that the membrane interaction of the PLM cytoplasmic domain is highly dependent on the lipid headgroup composition, and that the interaction with membranes containing physiological amounts of anionic phospholipids is rather weak. Structural models of the PLM/NKA interaction based on NMR measurements on anionic detergent micelles suggest that the cytoplasmic domain is retained at the membrane surface [19,21,22]. The highly charged micellar environment may not in this instance be a suitable proxy for a cell membrane bearing a much lower surface charge. We suggest a refinement to the recently proposed models, which allows PLM to populate several orientational and structural states in dynamic equilibrium. At one extreme the PLM cytoplasmic domain may orient approximately perpendicularly to the transmembrane region as depicted in the NMR models [19,21,22]. We hypothesize that the cytoplasmic domain is also free to move away from the membrane to a more upright orientation in contact with the NKA cytoplasmic domain close to the nucleotide site. Such an orientation could account for the effect of PLM_{38-72} on the sodium and nucleotide affinity of NKA. The effect of PLM phosphorylation on such a dynamic equilibrium is not known; phosphorylation reduces the affinity of the cytoplasmic domain for highly anionic lipid membranes, but this may have little overall effect in physiologically-charged membranes where the membrane affinity is already weak. Phosphorylation at S68 does not alter the depressed nucleotide and sodium affinity of NKA, yet phosphorylation alleviates the effect on V_{max} and also reduces the propensity of the PLM cytoplasmic domain to adopt an α-helical structure in 40% TFE. Together these observations suggest that phosphorylation of PLM has greater consequences for NKA-PLM interaction than for the interactions of PLM with the membrane surface.

Acknowledgements

The expert technical assistance of Ms. Angelina Damgaard is acknowledged. This work was supported by the British Heart Foundation (grant PG/06/138/21833).

References

[1] D.M. Bers, Calcium fluxes involved in control of cardiac myocyte contraction, Circ. Res. 87 (2000) 275–281.
[2] D.M. Bers, S. Despa, Cardiac myocytes Ca2+ and Na+ regulation in normal and failing hearts, J. Pharmacol. Sci. 100 (2006) 315–322.
[3] J.Y. Cheung, L.I. Rothblum, J.R. Moorman, A.L. Tucker, J.L. Song, B.A. Ahlers, L.L. Carl, J.F. Wang, X.Q. Zhang, Regulation of cardiac Na+/Ca2+ exchanger by phospholemman, Ann. NY Acad. Sci. 1099 (2007) 119–134.
[4] D.M. Bers, S. Despa, J. Bossuyt, Regulation of Ca2+ and Na+ in normal and failing cardiac myocytes, Ann. NY Acad. Sci. 1080 (2006) 165–177.
[5] A.L. Tucker, J.L. Song, X.Q. Zhang, J.F. Wang, B.A. Ahlers, L.L. Carl, J.P. Mounsey, J.R. Moorman, L.I. Rothblum, J.Y. Cheung, Altered contractility and [Ca2+](i) homeostasis in phospholemman-deficient murine myocytes: role of Na+/Ca2+ exchange, Am. J. Physiol. Heart Circ. Physiol. 291 (2006) H2199–H2209.
[6] G. Crambert, M. Fuzesi, H. Garty, S. Karlish, K. Geering, Phospholemman (FXYD1) associates with Na, K-ATPase and regulates its transport properties, Proc. Natl Acad. Sci. USA 99 (2002) 11476–23367.
[7] X.-Q. Zhang, A. Qureshi, J. Song, L.L. Carl, Q. Tian, R.C. Stahl, D.J. Carey, L.I. Rothblum, J.Y. Cheung, Phospholemman modulates Na+/Ca2+ exchange in adult rat cardiac myocytes, Am. J. Physiol. Heart Circ. Physiol. 284 (2003) H225–H233.
[8] L. Chen, C. Lo, R. Numann, M. Cuddy, Characterization of the human and rat phospholemman (PLM) cDNAs and localization of the human PLM gene to chromosome 19q13.1, Genomics 41 (1997) 435–443.

[9] K. Sweadner, E. Rael, The FXYD gene family of small ion transport regulators or channels: cDNA sequence, protein signature sequence, and expression, Genomics 68 (2000) 41–56.
[10] P. Beguin, G. Crambert, F. Monnet-Tschudi, M. Uldry, J.-D. Horisberger, H. Garty, K. Geering, FXYD7 is a brain-specific regulator of Na,K-ATPase alpha}1-{beta isozymes, EMBO J. 21 (2002) 3264–3273.
[11] P. Beguin, G. Crambert, S. Guennoun, H. Garty, J.-D. Horisberger, K. Geering, CHIF, a member of the FXYD protein family, is a regulator of Na, K-ATPase distinct from the {gamma}-subunit, EMBO J. 20 (2001) 3993–4002.
[12] P. Beguin, X.Y. Wang, D. Firsov, A. Puoti, D. Claeys, J.D. Horisberger, K. Geering, The gamma subunit is a specific component of the Na,K-ATPase and modulates its transport function, EMBO J. 16 (1997) 4250–4260.
[13] F. Cornelius, Y.A. Mahmmoud, Functional modulation of the sodium pump: the regulatory proteins "Fixit", News Physiol. Sci. 18 (2003) 119–124.
[14] C. Li, A. Grosdidier, G. Crambert, J.-D. Horisberger, O. Michielin, K. Geering, Structural and functional interaction sites between Na, K-ATPase and FXYD proteins, J. Biol. Chem. 279 (2004) 38895–38902.
[15] D. Pavlovic, W. Fuller, M.J. Shattock, The intracellular region of FXYD1 is sufficient to regulate cardiac Na/K ATPase, FASEB J. 21 (2007) 1539–1546.
[16] C. Palmer, B. Scott, L. Jones, Purification and complete sequence determination of the major plasma membrane substrate for cAMP-dependent protein kinase and protein kinase C in myocardium, J. Biol. Chem. 266 (1991) 11126.
[17] J.P. Mounsey, J.E. John III, S.M. Helmke, E.W. Bush, J. Gilbert, A.D. Roses, M.B. Perryman, L.R. Jones, J.R. Moorman, Phospholemman is a substrate for myotonic dystrophy protein kinase, J. Biol. Chem. 275 (2000) 23362–23367.
[18] P. Teriete, C.M. Franzin, J. Choi, F.M. Marassi, Structure of the Na, K-ATPase regulatory protein FXYD1 in micelles, Biochemistry 46 (2007) 6774–6783.
[19] C.M. Franzin, X.M. Gong, P. Teriete, F.M. Marassi, Structures of the FXYD regulatory proteins in lipid micelles and membranes, J. Bioenerg. Biomembr. 39 (2007) 379–383.
[20] P. Teriete, K. Thai, J. Choi, F.M. Marassi, Effects of PKA phosphorylation on the conformation of the Na, K-ATPase regulatory protein FXYD1, Biochim. Biophys. Acta 1788 (2009) 2462–2470.
[21] C.M. Franzin, X.M. Gong, K. Thai, J.H. Yu, F.M. Marassi, NMR of membrane proteins in micelles and bilayers: the FXYD family proteins, Methods 41 (2007) 398–408.
[22] C.M. Franzin, J.H. Yu, K. Thai, J. Choi, F.M. Marassi, Correlation of gene and protein structures in the FXYD family proteins, J. Mol. Biol. 354 (2005) 743–750.
[23] J. Clayton, E. Hughes, D. Middleton, The cytoplasmic domains of phospholamban and phospholemman associate with phospholipid membrane surfaces, Biochemistry 44 (2005) 17016–17026.
[24] P.L. Jørgensen, Purification and characterization of (Na+ + K+)-ATPase: III. Purification from the outer medulla of mammalian kidney after selective removal of membrane components by sodium dodecyl sulphate, Biochim. Biophys. Acta 356 (1974) 36–52.
[25] I. Klodos, M. Esmann, R.L. Post, Large-scale preparation of sodium-potassium ATPase from kidney outer medulla, Kidney Int. 62 (2002) 2097–2100.
[26] M. Esmann, ATPase and phosphatase activity of the Na, K-ATPase; molar and specific activity, protein determinations, Meth. Enzymol. 156 (1988) 105–115.
[27] C.H. Fiske, Y. Subbarow, The colorimetric determination of phosphorus, J. Biol. Chem. 66 (1925) 375–400.
[28] E.S. Baginski, P.P. Foà, B. Zak, Microdetermination of inorganic phosphate, phospholipids, and total phosphate in biologic materials, Clin. Chem. 13 (1967) 326–332.
[29] N.U. Fedosova, P. Champeil, M. Esmann, Nucleotide binding to Na,K-ATPase: the role of electrostatic interactions, Biochemistry 41 (2002) 1267–1273.
[30] T. Abraham, R. Lewis, R.S. Hodges, R.N. McElhaney, Isothermal titration calorimetry studies of the binding of a rationally designed analogue of the antimicrobial peptide gramicidin S to phospholipid bilayer membranes, Biochemistry 44 (2005) 2103–2112.
[31] K.R. Oldenburg, R.F. Epand, A. Dorfani, K. Vo, H. Selick, R.M. Epand, Conformational studies on analogs of recombinant parathyroid hormone and their interactions with phospholipids, J. Biol. Chem. 271 (1996) 17582–17591.
[32] J. Seelig, Titration calorimetry of lipid–peptide interactions, Biochim. Biophys. Acta 1331 (1997) 103–116.
[33] J.M. Scholtz, Q. Hong, E.J. York, J.M. Stewart, R.L. Baldwin, Parameters of helix-coil transition theory for alanine-based peptides of varying chain lengths in water, Biopolymers 31 (1991) 1463–1470.
[34] T. Gullion, J. Schaefer, Rotational-echo double-resonance NMR, J. Magn. Reson. 81 (1989) 196–200.
[35] A.E. Bennett, C.M. Rienstra, M. Auger, K.V. Lakshmi, R.G. Griffin, J. Chem. Phys. 103 (1995) 6951.
[36] H. Binder, G. Lindblom, Charge-dependent translocation of the Trojan peptide penetratin across lipid membranes, Biophys. J. 85 (2003) 982–995.
[37] H. Binder, G. Lindblom, Interaction of the Trojan peptide penetratin with anionic lipid membranes—a calorimetric study, Phys. Chem. Chem. Phys. 5 (2003) 5108–5117.
[38] J. Seelig, Thermodynamics of lipid–peptide interactions, Biochim. Biophys. Acta-Biomembr. 1666 (2004) 40–50.
[39] E. Breukink, P. Ganz, B. de Kruijff, J. Seelig, Binding of nisin Z to bilayer vesicles as determined with isothermal titration calorimetry, Biochemistry 39 (2000) 10247–10254.
[40] T. Wieprecht, O. Apostolov, J. Seelig, Binding of the antibacterial peptide magainin 2 amide to small and large unilamellar vesicles, Biophys. Chem. 85 (2000) 187–198.
[41] J. Depont, A. Vanprooijenvaneeden, S.L. Bonting, Role of negatively charged phospholipids in highly purified (Na+ + K+)-Atpase from rabbit kidney outer medulla: 39. Studies on (Na+ + K+)-activated Atpase, Biochim. Biophys. Acta 508 (1978) 464–477.
[42] C.M. Franzin, P. Teriete, F.M. Marassi, Structural similarity of a membrane protein in micelles and membranes, J. Am. Chem. Soc. 129 (2007) 8078–8079.
[43] C.M. Franzin, P. Teriete, F.M. Marassi, Membrane orientation of the Na,K-ATPase regulatory membrane protein CHIF determined by solid-state NMR, Magn. Reson. Chem. 45 (2007) S192–S197.
[44] S.G. Patching, A.R. Brough, R.B. Herbert, J.A. Rajakarier, P.J.F. Henderson, D.A. Middleton, Substrate affinities for membrane transport proteins determined by C-13 cross-polarization magic-angle spinning nuclear magnetic resonance spectroscopy, J. Am. Chem. Soc. 126 (2004) 3072–3080.
[45] M. Esmann, A. Watts, D. Marsh, Spin label studies of lipid–protein interactions in Na,K-ATPase membranes from rectal glands of Squalus acanthias, Biochemistry 24 (1985).
[46] O. Toke, W.L. Maloy, S.J. Kim, J. Blazyk, J. Schaefer, Secondary structure and lipid contact of a peptide antibiotic in phospholipid bilayers by REDOR, Biophys. J. 87 (2004) 662–674.
[47] O. Toke, L. Cegelski, J. Schaefer, Peptide antibiotics in action: investigation of polypeptide chains in insoluble environments by rotational-echo double resonance, Biochim. Biophys. Acta-Biomembr. 1758 (2006) 1314–1329.
[48] B.N. Kholodenko, J.B. Hoek, H.V. Westerhoff, Why cytoplasmic signalling proteins should be recruited to cell membranes, Trends Cell Biol. 10 (2000) 173–178.
[49] J. Song, X. Zhang, L.L. Carl, L.I. Rothblum, J.Y. Cheung, Phospholemman (PLM) overexpression affects contractile function in rat myocytes, Biophys. J. 82 (2002) 597A.
[50] J. Bossuyt, X. Ai, J.R. Moorman, S.M. Pogwizd, D.M. Bers, Expression and phosphorylation of the Na-pump regulatory subunit phospholemman in heart failure, Circ. Res. 97 (2005) 558–565.
[51] B.A. Ahlers, X.-Q. Zhang, J.R. Moorman, L.I. Rothblum, L.L. Carl, J. Song, J. Wang, L.M. Geddis, A.L. Tucker, J.P. Mounsey, J.Y. Cheung, Identification of an endogenous inhibitor of the cardiac Na+/Ca2+ exchanger, phospholemman, J. Biol. Chem. 280 (2005) 19875–19882.
[52] J. Song, X.-Q. Zhang, B.A. Ahlers, L.L. Carl, J. Wang, L.I. Rothblum, R.C. Stahl, J.P. Mounsey, A.L. Tucker, J.R. Moorman, J.Y. Cheung, Serine 68 of phospholemman is critical in modulation of contractility, [Ca2+]i transients, and Na+/Ca2+ exchange in adult rat cardiac myocytes, Am. J. Physiol. Heart Circ. Physiol. 288 (2005) H2342–H2354.
[53] J.F. Wang, X.Q. Zhang, B.A. Ahlers, L.L. Carl, J.L. Song, L.I. Rothblum, R.C. Stahl, D.J. Carey, J.Y. Cheung, Cytoplasmic tail of phospholemman interacts with the intracellular loop of the cardiac Na+/Ca2+ exchanger, J. Biol. Chem. 281 (2006) 32004–32014.
[54] G. Crambert, M. Fuzesi, H. Garty, S. Karlish, K. Geering, Phospholemman (FXYD1) associates with Na, K-ATPase and regulates its transport properties, Proc. Natl Acad. Sci. USA 99 (2002) 11476–11481.
[55] L.G. Jia, C. Donnet, R.C. Bogaev, R.J. Blatt, C.E. McKinney, K.H. Day, S.S. Berr, L.R. Jones, J.R. Moorman, K.J. Sweadner, A.L. Tucker, Hypertrophy, increased ejection fraction, and reduced Na-K-ATPase activity in phospholemman-deficient mice, Am. J. Physiol. Heart Circ. Physiol. 288 (2005) H1982–H1988.
[56] I.M.C. Dixon, T. Hata, N.S. Dhalla, Sarcolemmal Na+-K+-Atpase activity in congestive-heart-failure due to myocardial-infarction, Am. J. Physiol. 262 (1992) C664–C671.
[57] X.Q. Zhang, J.R. Moorman, B.A. Ahlers, L.L. Carl, D.E. Lake, J.L. Song, J.P. Mounsey, A.L. Tucker, Y.M. Chan, L.I. Rothblum, R.C. Stahl, D.J. Carey, J.Y. Cheung, Phospholemman overexpression inhibits Na+-K+-ATPase in adult rat cardiac myocytes: relevance to decreased Na+ pump activity in postinfarction myocytes, J. Appl. Physiol. 100 (2006) 212–220.
[58] J. Bossuyt, X. Ai, J.R. Moorman, S.M. Pogwizd, D.M. Bers, Expression and phosphorylation of the Na-pump regulatory subunit phospholemman in heart failure, Circ. Res. 97 (2005) 558–565.
[59] J. Neumann, R. Maas, P. Boknik, L.R. Jones, N. Zimmermann, H. Scholz, Pharmacological characterization of protein phosphatase activities in preparations from failing human hearts, J. Pharmacol. Exp. Ther. 289 (1999) 188–193.